The EMBO Journal (2012) 31, 1865–1878 | © 2012 European Molecular Biology Organization | All Rights Reserved 0261-4189/12
www.embojournal.org

THE EMBO JOURNAL

RNF8- and RNF168-dependent degradation of KDM4A/JMJD2A triggers 53BP1 recruitment to DNA damage sites

Frédérick A Mallette[1,2], Francesca Mattiroli[3], Gaofeng Cui[4], Leah C Young[5], Michael J Hendzel[5], Georges Mer[4], Titia K Sixma[3] and Stéphane Richard[1,2,*]

[1]Terry Fox Molecular Oncology Group and the Bloomfield Center for Research on Aging, Sir Mortimer B. Davis Jewish General Hospital, Lady Davis Institute for Medical Research, Montréal, Québec, Canada, [2]Department of Medicine and Oncology, McGill University, Montréal, Québec, Canada, [3]Division of Biochemistry, Netherlands Cancer Institute, Amsterdam, The Netherlands, [4]Department of Biochemistry and Molecular Biology, Mayo Clinic College of Medicine, Rochester, MN, USA and [5]Department of Oncology, University of Alberta, Edmonton, Alberta, Canada

In response to DNA damage, cells initiate complex signalling cascades leading to growth arrest and DNA repair. The recruitment of 53BP1 to damaged sites requires the activation of the ubiquitination cascade controlled by the E3 ubiquitin ligases RNF8 and RNF168, and methylation of histone H4 on lysine 20. However, molecular events that regulate the accessibility of methylated histones, to allow the recruitment of 53BP1 to DNA breaks, are unclear. Here, we show that like 53BP1, the JMJD2A (also known as KDM4A) tandem tudor domain binds dimethylated histone H4K20; however, JMJD2A is degraded by the proteasome following the DNA damage in an RNF8-dependent manner. We demonstrate that JMJD2A is ubiquitinated by RNF8 and RNF168. Moreover, ectopic expression of JMJD2A abrogates 53BP1 recruitment to DNA damage sites, indicating a role in antagonizing 53BP1 for methylated histone marks. The combined knockdown of JMJD2A and JMJD2B significantly rescued the ability of RNF8- and RNF168-deficient cells to form 53BP1 foci. We propose that the RNF8-dependent degradation of JMJD2A regulates DNA repair by controlling the recruitment of 53BP1 at DNA damage sites.

The EMBO Journal (2012) **31,** 1865–1878. doi:10.1038/emboj.2012.47; Published online 28 February 2012
Subject Categories: proteins; genome stability & dynamics
Keywords: 53BP1; JMJD2A; RNF168; RNF8; tudor

Introduction

DNA damage recognition and repair in the context of chromatin constitute a challenge for protein accessibility and recruitment to DNA damage sites. Multiple histone post-translational modifications (phosphorylation, acetylation, sumoylation, ubiquitination and methylation) contribute to the efficient formation of protein complexes to trigger the DNA damage response (van Attikum and Gasser, 2009). Following DNA damage, the Mre11/Rad50/Nbs1 (MRN) complex recognizes the break and contributes to the activation of ATM leading to the phosphorylation of H2AX across kilobases of DNA surrounding the damaged site (Shroff *et al*, 2004). A cascade of protein relocalization is then triggered by the binding of the mediator protein MDC1 to phosphorylated H2AX (γH2AX) through its BRCT domain (Stucki *et al*, 2005). MDC1 then amplifies the DNA damage signalling response by coordinating the assembly of checkpoint and repair proteins (Goldberg *et al*, 2003; Lou *et al*, 2003, 2006; Stewart *et al*, 2003; Bekker-Jensen *et al*, 2005). The phospho-dependent interaction of MDC1 with the E3 ubiquitin ligase RNF8 allows the formation of K63-linked polyubiquitin chains on histones surrounding the damaged site (Huen *et al*, 2007; Kolas *et al*, 2007; Mailand *et al*, 2007). The RNF168 and HERC2 ubiquitin ligases have also been described to contribute to the formation of ubiquitin conjugates on H2A and H2AX at breaks (Doil *et al*, 2009; Stewart *et al*, 2009; Bekker-Jensen *et al*, 2010). This ubiquitination cascade regulated by RNF8, RNF168 and HERC2 is responsible for the localization of both RAP80/BRCA1 and 53BP1 at DNA damage sites (Huen *et al*, 2007; Kolas *et al*, 2007; Mailand *et al*, 2007; Wang and Elledge, 2007; Doil *et al*, 2009; Stewart *et al*, 2009; Bekker-Jensen *et al*, 2010). While RAP80 recruitment is mediated through the binding of its ubiquitin-interacting motif (UIM) with K63-linked ubiquitin chains on histones, the RNF8-dependent mechanism leading to the formation of 53BP1 foci remains undefined. The role of methylation of histone H4 on lysine 20 in the recruitment of 53BP1 and the requirement of the 53BP1 tandem tudor domain are established (Sanders *et al*, 2004; Botuyan *et al*, 2006), but the link with RNF8-dependent ubiquitination is still unclear. RNF8-mediated ubiquitination of histones at damaged sites may alter chromatin structure, leading to the exposure of buried H4K20(me2) in stacked nucleosomes allowing recognition by the 53BP1 tandem tudor domain. However, since nucleosomes are already highly dynamic structures permitting protein access even to buried sites of chromatin (Li *et al*, 2005), an additional mechanism must lead to the exposure of H4K20(me2). The high abundance of H4K20(me2) in untreated cells suggest that this mark is usually inaccessible to 53BP1 (Schotta *et al*, 2008). The recruitment of the H4K20 methyltransferase MMSET at breaks may locally increase levels of H4K20(me2) (Pei *et al*, 2011), but it does not elucidate the requirement of RNF8 to form 53BP1 foci. Here, we show that the RNF8-mediated degradation of JMJD2A is required to expose H4K20(me2) for the recruitment of 53BP1 to DNA damage sites.

*Corresponding author. Segal Cancer Centre, Lady Davis Institute for Medical Research, 3755 Côte Ste-Catherine Road, Montréal, Québec, Canada H3T 1E2. Tel.: +1 514 340 8260 ext 4470; Fax: +1 514 340 7502; E-mail: stephane.richard@mcgill.ca

Received: 22 December 2011; accepted: 7 February 2012; published online: 28 February 2012

©2012 European Molecular Biology Organization

Results

JMJD2A tandem tudor domain tightly binds to H4K20(me2)

The lysine demethylase JMJD2A catalyses the removal of both di- and tri-methylated H3K9 and H3K36 (Cloos *et al*, 2006; Klose *et al*, 2006; Whetstine *et al*, 2006; Couture *et al*, 2007; Ng *et al*, 2007). It possesses an N-terminal JmjN and catalytic JmjC domain, two PHD domains and a tandem tudor domain (Figure 1A and B). The C-terminal tandem tudor domain likely functions as a chromatin recruitment binding module, as it can bind to H3K4(me3) and H4K20(me2/3) (Huang *et al*, 2006; Kim *et al*, 2006; Lee *et al*, 2008). Like 53BP1, JMJD2A also binds H4K20(me2) (Figure 1C).

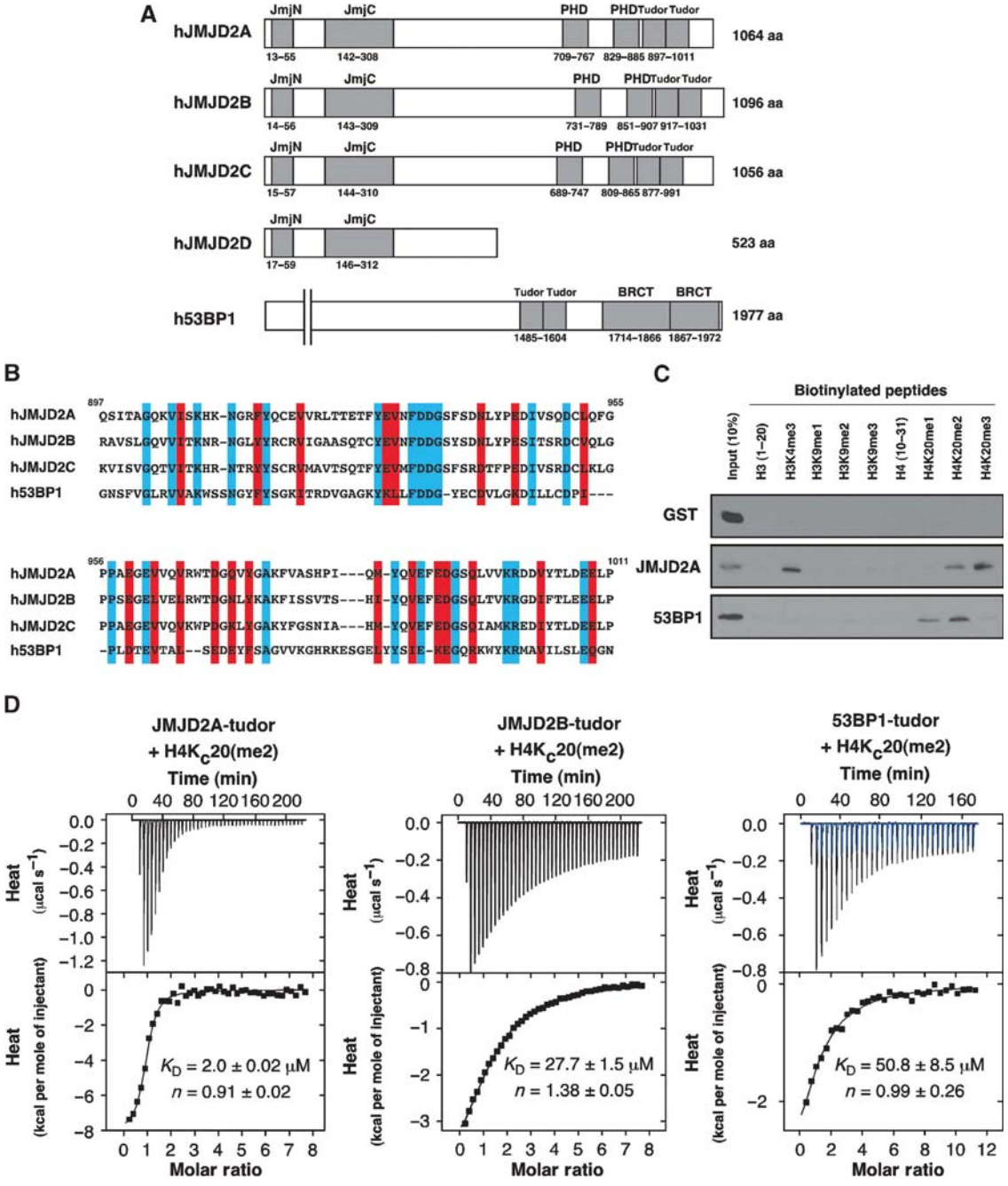

Figure 1 The tandem tudor domains of JMJD2A and JMJD2B bind H4K20(me2) with high affinity. (**A**) Domain structure of the different members of the JMJD2 family of lysine demethylases and 53BP1. (**B**) Sequence alignment of the tandem tudor domains of human JMJD2A, JMJD2B, JMJD2C and 53BP1 using TCoffee. Amino acids highlighted in blue show perfect conservation while red denotes amino acids corresponding to functional conservation. (**C**) Biotinylated peptides immobilized on streptavidin beads were used to pulldown GST-purified JMJD2A and 53BP1 tandem tudor domains. (**D**) Titrations of JMJD2A-tudor, JMJD2B-tudor and 53BP1-tudor with H4K$_C$20(me2) (residues 12–25). The integrated heat measurements from raw titration data and curve fitting with a standard one-site binding model are shown for each experiment. K_D and stoichiometry (n) values are indicated with the associated standard deviations determined by non-linear least squares fitting. The heat of dilution of the H4K$_C$20(me2) peptide is shown in blue, overlaid to the 53BP1-tudor titration signal. Note that the K_D of H4K$_C$20(me2) for 53BP1-tudor is about twice that of H4K20(me2).

 ©2012 European Molecular Biology Organization

Recently, a novel methyltransferase, MMSET, has been shown to locally increase the methylation of H4K20 at breaks (Pei *et al*, 2011). It has also been proposed that changes in the chromatin structure expose these methyl marks leading to the recruitment of 53BP1 (Sanders *et al*, 2004; Botuyan *et al*, 2006). However, the possibility that proteins masking accessibility to H4K20(me2) might be regulated by the DNA damage response to reveal the methyl mark has remained unexplored. We first determined the relative affinities of the tandem tudor domains of JMJD2A, JMJD2B and 53BP1 for H4K20(me2). The JMJD2A-tudor and JMJD2B-tudor bound H4K20(me2) with a K_D about 25 and 2 times tighter, respectively, compared with 53BP1-tudor, as shown by isothermal titration calorimetry (ITC) (Figure 1D). This suggests that JMJD2A and JMJD2B tightly bind to H4K20(me2) and may compete *in vivo* for accessibility to H4K20(me2).

JMJD2A protein is degraded after DNA damage

To determine whether the expression levels of JMJD2A are regulated following DNA damage, we treated U2OS cells with the chemotherapeutic drug doxorubicin and monitored JMJD2A protein expression. DNA damage, as monitored by the appearance of γH2AX, led to significant decrease in JMJD2A and JMJD2B expression levels, but not of the other JMJD2 members, JMJD2C and JMJD2D (Figure 2A). JMJD2A protein levels were also sensitive to other DNA damaging agents including ionizing radiation (IR) and UV (Figure 2B and C), and exogenous JMJD2A was also affected by doxorubicin treatment (Figure 2D). Using protein synthesis inhibitors, we observed a global JMJD2A reduction as early as 15 min after treatment with doxorubicin and defined the half-life of JMJD2A to be ∼45 min in the presence of doxorubicin, whereas it was >90 min in untreated cells (Figure 2E and F). The short half-life of JMJD2A after DNA damage correlates with the kinetics of recruitment of 53BP1 to DNA breaks in cells treated with doxorubicin where most of the cells harboured foci around 30 min (Supplementary Figure S1). At the chromatin level, the reduction of JMJD2A protein was even more dramatic where most of the protein was no longer associated with chromatin (Figure 2G). These results suggest that eviction of JMJD2A from chromatin occurs rapidly following DNA damage and that the global depletion of JMJD2A arise simultaneously or at later time points. The decreased stability of JMJD2A following DNA damage was ATM dependent, since treatment of the cells with the ATM inhibitor KU-55933 abolished the DNA damage-induced degradation of JMJD2A (Supplementary Figure S2).

RNF8 and RNF168 ubiquitin ligases modulate JMJD2A degradation

To determine if JMJD2A can be modified by ubiquitination *in vivo*, we transfected U2OS cells with plasmids expressing HA–ubiquitin and Flag–JMJD2A. Cell extracts were subjected to immunoprecipitation with anti-flag antibody and immunoblotted using anti-HA or anti-flag. Co-expression of HA–ubiquitin and Flag–JMJD2A caused a dramatic increase in ubiquitinated JMJD2A that was not observed in the absence of HA–ubiquitin (Figure 3A). Furthermore, treatment with the proteasome inhibitor MG132 led to JMJD2A stabilization and increased levels of its ubiquitination (Figure 3A). MG132 also stabilized JMJD2A after DNA damage (Figure 3B). Stabilization of JMJD2A by the inhibition of the proteasome caused a marked reduction in Chk2 phosphorylation, a hallmark of defective 53BP1 recruitment (Wang *et al*, 2002; Figure 3B).

The RNF8-dependent ubiquitination cascade regulates the recruitment of DNA damage mediators to DNA breaks by catalysing the addition of ubiquitin moieties to H2A (Huen *et al*, 2007; Kolas *et al*, 2007; Mailand *et al*, 2007; Wang and Elledge, 2007; Doil *et al*, 2009; Stewart *et al*, 2009; Bekker-Jensen *et al*, 2010). To determine the role of RNF8 in JMJD2A protein stability after DNA damage, we co-expressed increasing amounts of RNF8 with JMJD2A in U2OS cells. Higher levels of RNF8 expression led to a reduction in JMJD2A protein levels (Figure 3C). Conversely, RNF8 knockdown using two different siRNAs resulted in JMJD2A protein accumulation (Figure 3D), with no change in JMJD2A mRNA levels (Figure 3E), and abrogated JMJD2A degradation following DNA damage (Figure 3F). RNF8 knockdown also led to an increase of JMJD2B protein but not of JMJD2C or JMJD2D (Figure 3D), suggesting that RNF8 plays a key role in destabilizing JMJD2A and JMJD2B. We next performed an *in vitro* ubiquitination assay to determine the ability of RNF8 to directly mediate the ubiquitination of JMJD2A. We used recombinant proteins containing the JMJD2A N-terminal (1–532) or C-terminal (533–1064) portion tagged with flag and GST. A typical ubiquitination laddering pattern was observed when the N- and C-terminal JMJD2A were incubated with either full-length RNF8 or its RING domain, indicating that JMJD2A is a direct substrate of RNF8 (Figure 3G). Mutation at the E2-binding interface of the RING domain of RNF8 ($RNF8^{I405A}$) greatly diminished its ability to mediate the ubiquitination of JMJD2A (Figure 3G).

While it was initially considered that RNF8 preferentially mediates K63-linked ubiquitination (Figure 4A), we show that RNF8 and RNF168 are also capable of generating K48-linked ubiquitin chains leading to proteasomal degradation (Figure 4B), consistent with findings by Meerang *et al* (2011) and Plans *et al* (2006). Furthermore, we show that RNF8 stimulates the formation of K48-linked ubiquitin moieties on JMJD2A *in vivo*, as wild-type ubiquitin but not K48R-mutated ubiquitin could be used to ubiquitinate JMJD2A (Figure 4C). The mobility of JMJD2A as assayed by fluorescence recovery after photobleaching (FRAP) was increased in the presence of RNF8, suggesting that ubiquitination by RNF8 also controls JMJD2A association with chromatin (Supplementary Figure S3).

RNF8 is part of a cascade of ubiquitin ligases, including RNF168, contributing to the DNA damage response (Huen *et al*, 2007; Kolas *et al*, 2007; Mailand *et al*, 2007; Wang and Elledge, 2007; Doil *et al*, 2009; Stewart *et al*, 2009). In U2OS cells, co-expression of RNF168 with JMJD2A, like RNF8, led to decreased JMJD2A levels (Figure 5A). As a control, expression of the RING domain-containing E3 ubiquitin ligase XIAP had no effect on JMJD2A protein levels (Figure 5A). Depletion of RNF168 led to the accumulation of JMJD2A and JMJD2B proteins , but not of JMJD2C or JMJD2D (Figure 5B). RNF168 was able to directly ubiquitinate the N-terminal and weakly the C-terminal of JMJD2A *in vitro* whereas a RING domain mutant could not (Figure 5C). Our findings suggest that the DNA damage-induced JMJD2A degradation is RNF8 and RNF168 dependent and that JMJD2A is a direct substrate of RNF8 and RNF168.

©2012 European Molecular Biology Organization

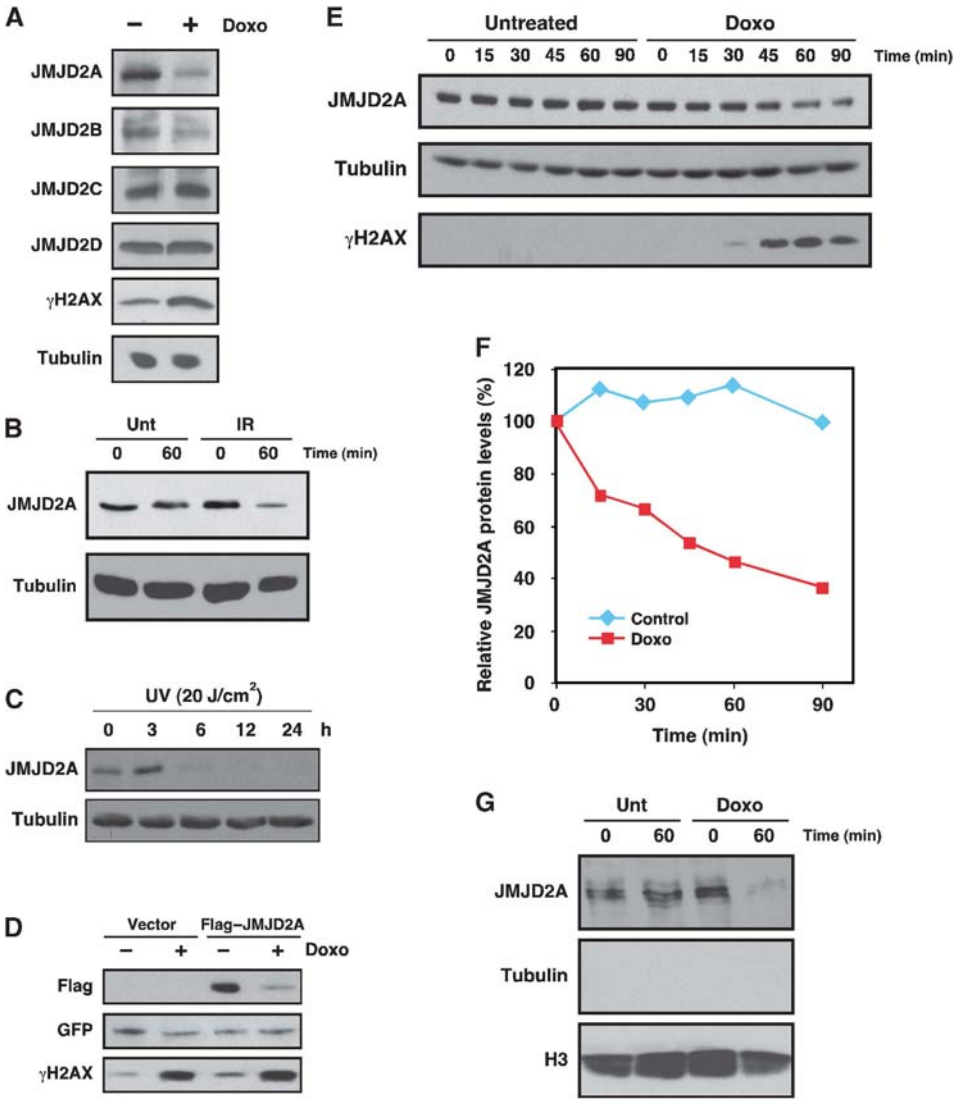

Figure 2 DNA damage triggers degradation of the lysine demethylase JMJD2A. (**A**) Immunoblot analysis of the JMJD2 family members in U2OS left untreated or treated with 1 μM doxorubicin (doxo) for 12 h. (**B**) Protein stability of JMJD2A is affected by IR. U2OS cells were treated with cycloheximide and chloramphenicol for 1 h then exposed to IR (10 Gy). (**C**) Immunoblot analysis of JMJD2A in U2OS cells exposed to UV (20 J/cm^2). (**D**) Immunoblot analysis of U2OS cells transfected with the empty vector or pLPC Flag–JMJD2A using FUGENE6 and treated with 1 μM doxorubicin for 12 h. (**E**) JMJD2A protein half-life measurement by immunoblotting in U2OS cells treated or not with 2 μM doxorubicin (doxo) as described in Materials and methods. (**F**) The quantification of the results of (**E**) is shown. (**G**) Protein stability of chromatin-associated JMJD2A in U2OS cells treated with cycloheximide and chloramphenicol for 1 h, and exposed to 2 μM doxorubicin for 60 min.

JMJD2A blocks the formation of 53BP1 foci after DNA damage

It is known that treatment of U2OS cells with proteasome inhibitors impairs the recruitment of RAP80/BRCA1 (Jacquemont and Taniguchi, 2007; Mailand *et al*, 2007) and 53BP1 (Jacquemont and Taniguchi, 2007; Mailand *et al*, 2007; Sakasai and Tibbetts, 2008; Supplementary Figure S4) to sites of DNA damage without affecting the dimethylation of H4K20 (Sakasai and Tibbetts, 2008). Treatment with MG132 also inhibits the recruitment at DNA breaks of a minimal focus-targeting fragment of 53BP1 spanning the tandem tudor domain, suggesting that proteasome inhibition or depletion of nuclear ubiquitin blocks an event required for the tudor domain recruitment (Sakasai and Tibbetts, 2008). We wanted to investigate the role of JMJD2A protein degradation in 53BP1 foci formation. To do this, we ectopically reconstituted the levels of JMJD2A after DNA damage to a level comparable to endogenous JMJD2A in untreated cells (Supplementary Figure S5) and examined the presence of γH2AX, MDC1 and 53BP1 at sites of DNA damage. Interestingly, the expression of Flag–JMJD2A prevented the recruitment of 53BP1 (Figure 6A), but not γH2AX (Supplementary Figure S6A) and MDC1 (Supplementary Figure S6B) at sites of DNA damage following IR (Figure 6B). As a control, we also detected a defect in 53BP1 recruitment at sites of DNA damage in cells treated with RNF8 siRNAs (Figure 6A and B), as previously reported (Huen *et al*, 2007; Kolas *et al*, 2007; Mailand *et al*, 2007). Similar results were obtained in cells treated with doxorubicin indicating that 53BP1 recruitment behaves the same way in cells treated with IR or doxorubicin (Supplementary Figure S7). Contrary to the silencing of RNF8, the expression of JMJD2A did not affect RAP80 foci

 ©2012 European Molecular Biology Organization

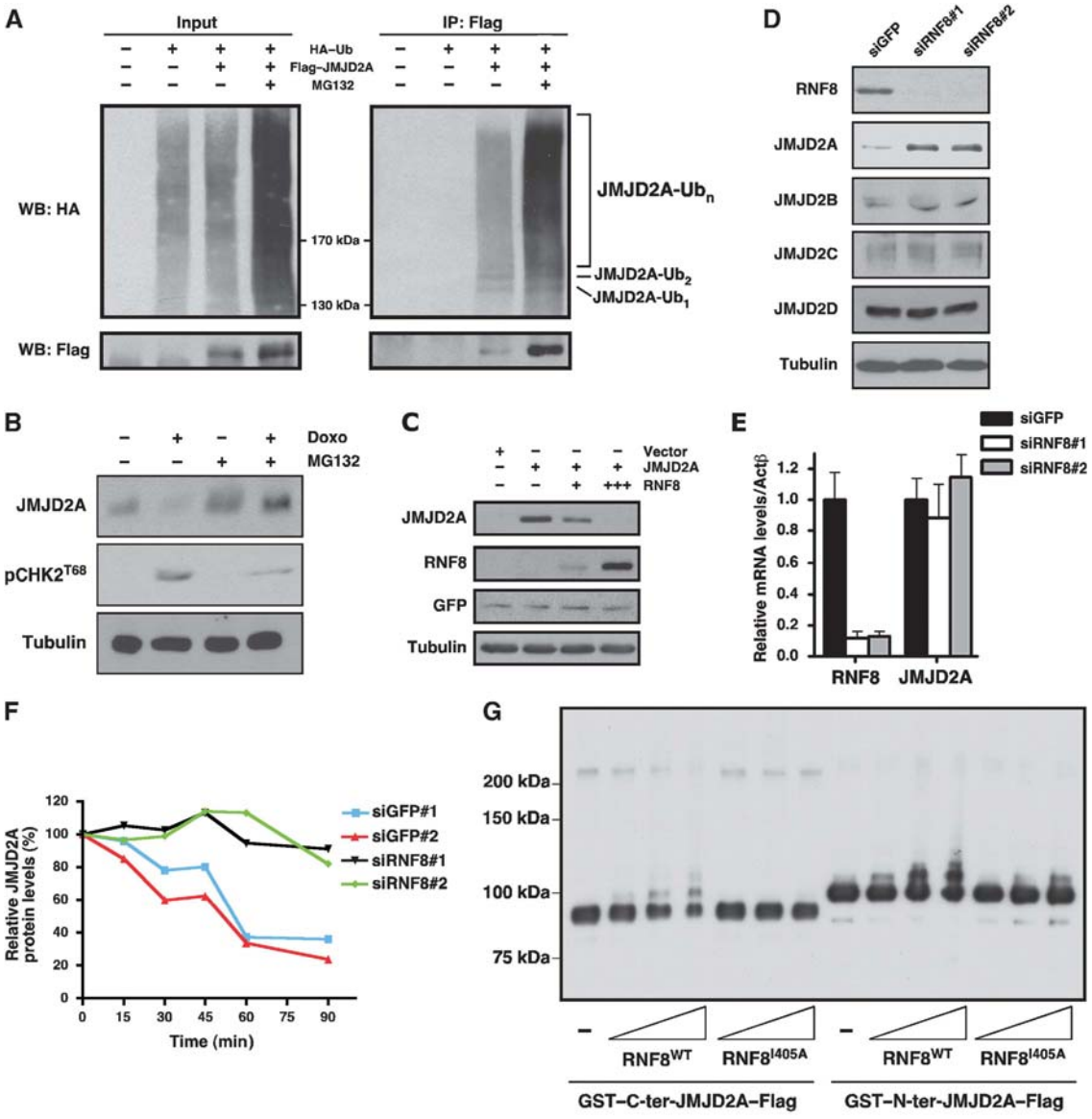

Figure 3 RNF8 directly ubiquitinates and regulates the stability of JMJD2A. (**A**) *In vivo* ubiquitination of JMJD2A in U2OS cells transfected with HA–ubiquitin and Flag–JMJD2A, and treated or not with 5 μM MG132. (**B**) Protein stability of JMJD2A in U2OS cells pre-treated with the proteasome inhibitor MG132 (5 μM) for 1 h, then treated with cycloheximide and chloramphenicol for 1 h, and exposed to 2 μM doxorubicin for 90 min. (**C**) JMJD2A protein levels in U2OS cells transfected with plasmids expressing Flag–JMJD2A and increasing amounts of RNF8. GFP was used to monitor transfection efficiency. (**D**) JMJD2 family members protein levels in U2OS cells transfected with siGFP or siRNAs against RNF8. (**E**) Relative mRNA levels using RT–qPCR for RNF8 and JMJD2A in U2OS cells transfected with GFP or RNF8 siRNAs using Lipofectamine RNAiMAX. (**F**) Protein stability of JMJD2A in U2OS cells transfected with siGFP or siRNF8, pre-treated with cycloheximide and chloramphenicol for 1 h and then treated with 2 μM doxorubicin. (**G**) The Flag–GST-tagged JMJD2A C- and N-terminal regions were used as substrates for ubiquitination by purified RNF8 wild-type or RING domain mutant RNF8^{I405A} in the presence of E1 (Uba1), E2 (UbcH5c) and ubiquitin. Increasing concentrations (0.1, 0.3 or 0.9 μM) of RNF8 or RNF8^{I405A} were used. The ubiquitination reactions were analysed by anti-flag immunoblotting.

formation, suggesting that RNF8 engages two independent pathways to recruit RAP80 and 53BP1 (Figure 6C). The inability to efficiently recruit 53BP1 to DNA breaks leads to defects in the phosphorylation of Chk2 at threonine 68 (Wang *et al*, 2002). Ectopic expression of JMJD2A also caused a significant reduction in the phosphorylated form of Chk2 at threonine 68 as expected in cells with 53BP1 foci defects (Figure 6D). The closely related JMJD2B, whose expression level is also sensitive to DNA damage (Figure 2A), but not JMJD2C and JMJD2D, also blocked the formation of 53BP1 foci (Figure 6E and F; Supplementary Figure S8), indicating that the other members of the JMJD2 family harbouring a tandem tudor domain may also regulate 53BP1 recruitment. As a control, another H4K20(me2) binding protein, PHF20, was overexpressed in the cells. The displacement of 53BP1 from DNA damage foci was not observed following expression of PHF20, suggesting that the effect is specific to JMJD2A/B (Supplementary Figure S9). PHF20, like 53BP1 and JMJD2A, has specificity for H4K20me2 but lower affinity than 53BP1 and JMJD2A (GM, personal communication); and therefore, unlike JMJD2A, PHF20 cannot efficiently compete with 53BP1 for binding H4K20me2.

©2012 European Molecular Biology Organization

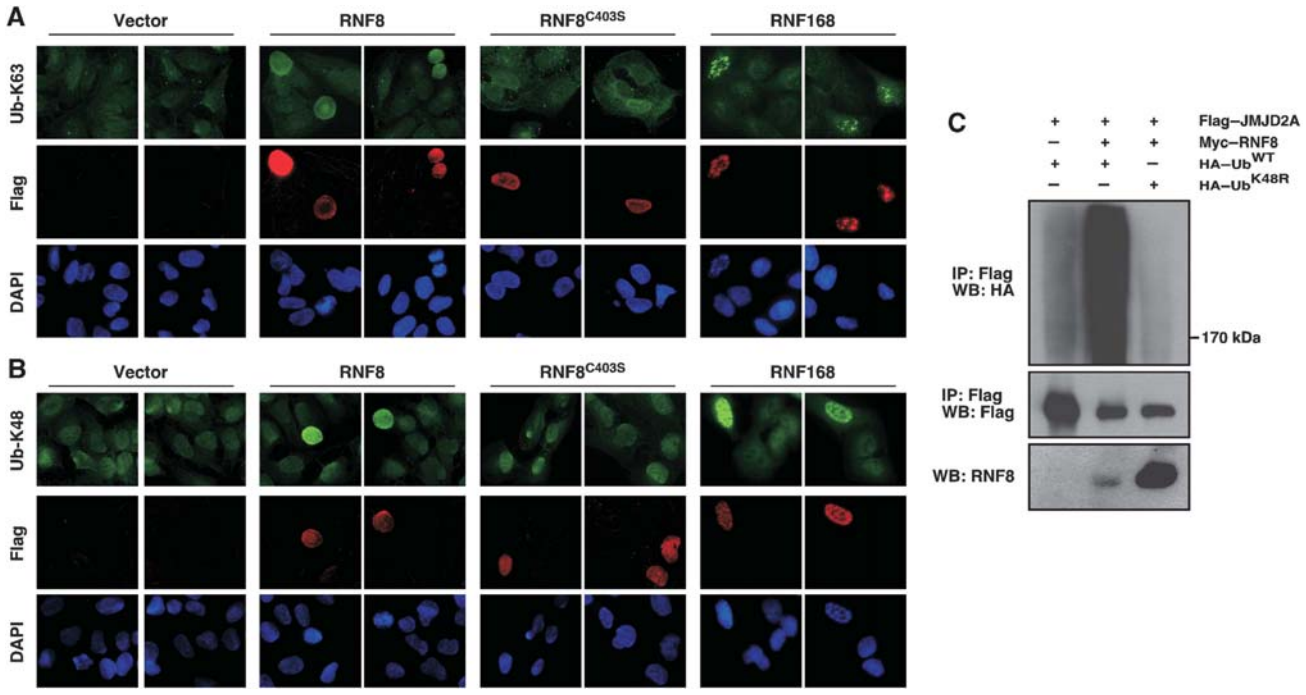

Figure 4 RNF8 stimulates the formation of K48-linked ubiquitin chains on JMJD2A. Indirect immunofluorescence of K63- (**A**) and K48-linked ubiquitin (**B**) in U2OS cells transfected with Flag–RNF8 or Flag–RNF168. (**C**) *In vivo* ubiquitination of JMJD2A in U2OS cells transfected with Flag–JMJD2A, myc–RNF8 and HA–Ub^{WT} or the mutant ubiquitin HA-Ub^{K48R}, and treated with 5 μM MG132 for 4 h.

The blockage of 53BP1 foci formation by JMJD2A suggests two possible mechanisms by which JMJD2A controls 53BP1 recruitment: either the catalytic activity of JMJD2A is required for the demethylation of histone marks other than H4K20(me2), or the JMJD2A tandem tudor domain competes with the 53BP1 tandem tudor domain for methylated histones. To discriminate between these two possible mechanisms, we generated an amino-acid substitution within the JMJD2A JmjC catalytic domain (JMJD2A^{H188A}) known to abrogate demethylase activity (Whetstine *et al*, 2006). We also substituted aspartic acid at position 939 to an arginine in the tandem tudor domain (JMJD2A^{D939R}) to disrupt binding to H4K20(me2/3) (Lee *et al*, 2008). Expression plasmids encoding the JMJD2A mutant proteins were transfected in U2OS cells and assayed for 53BP1 recruitment at DNA damage sites following IR. Like wild-type JMJD2A, the expression of JMJD2A^{H188A} prevented 53BP1 recruitment (Figure 7A and B; Supplementary Figure S10), indicating that the demethylase activity is not required. Interestingly, compromising the JMJD2A tandem tudor domain significantly re-established the recruitment of 53BP1 (Figure 7A and B; Supplementary Figure S10). The expression of JMJD2A^{D939R} led to a partial rescue of 53BP1 foci formation as this mutant retains some ability to bind H4K20(me2/3) (Lee *et al*, 2008). These results suggest that the JMJD2A tandem tudor domain blocks the accessibility of 53BP1 to H4K20(me2) in damaged and undamaged cells.

Since JMJD2A had first been described as a transcriptional repressor (Zhang *et al*, 2005; Klose *et al*, 2006), we examined the possibility that JMJD2A regulates 53BP1 expression or the 53BP1 recruiting methyl mark H4K20(me2). U2OS cells were stably infected with retroviruses expressing Flag–JMJD2A or an empty control vector and the 53BP1 protein expression and histone methyl marks were examined by immunoblotting. The ectopic expression of JMJD2A did not alter 53BP1 protein expression, nor did it have an effect on the presence of H4K20(me2) (Figure 7C). However, as expected, both H3K9(me3) and H3K36(me3) were decreased with JMJD2A expression (Figure 7C). These findings show that JMJD2A does not regulate 53BP1 protein levels nor the dimethylation of H4K20 known to be implicated in its recruitment.

Combined depletion of JMJD2A and JMJD2B rescues 53BP1 foci in RNF8- and RNF168-depleted cells

To confirm the role of RNF8-mediated degradation of JMJD2A in the recruitment of 53BP1, we used siRNAs targeting the different JMJD2 family members to rescue the 53BP1 defects in siRNF8-treated cells. The knockdown of JMJD2A alone was insufficient to re-establish the formation of 53BP1 foci in RNF8-knockdown cells (Supplementary Figure S11A and B). However, the combined knockdown of JMJD2A and JMJD2B significantly rescued the defects caused by the absence of RNF8 (Figure 8A and B; Supplementary Figures S11 and S12). This recovery of 53BP1 foci was not observed when siJMJD2A was combined with siJMJD2C (Supplementary Figure S11A and B), a family member not regulated by DNA damage (Figure 2A) and unable to efficiently block 53BP1 foci formation (Figure 6E and F). Furthermore, the combined knockdown of JMJD2A and JMJD2B also rescued the formation of 53BP1 foci in RNF168-depleted cells (Figure 8C and D). Depletion of JMJD2A/B in RNF8- and RNF168-deficient cells leads to the recruitment of 53BP1 at foci rather than on the entire chromosome, as there are other factors such as MMSET that are required to coordinate 53BP1 recruitment (Pei *et al*, 2011). We also performed the combined knockdown of JMJD2A and JMJD2B in undamaged cells and we noticed a significant increase of 53BP1 foci consistent with the few double-strand breaks observed in untreated

 ©2012 European Molecular Biology Organization

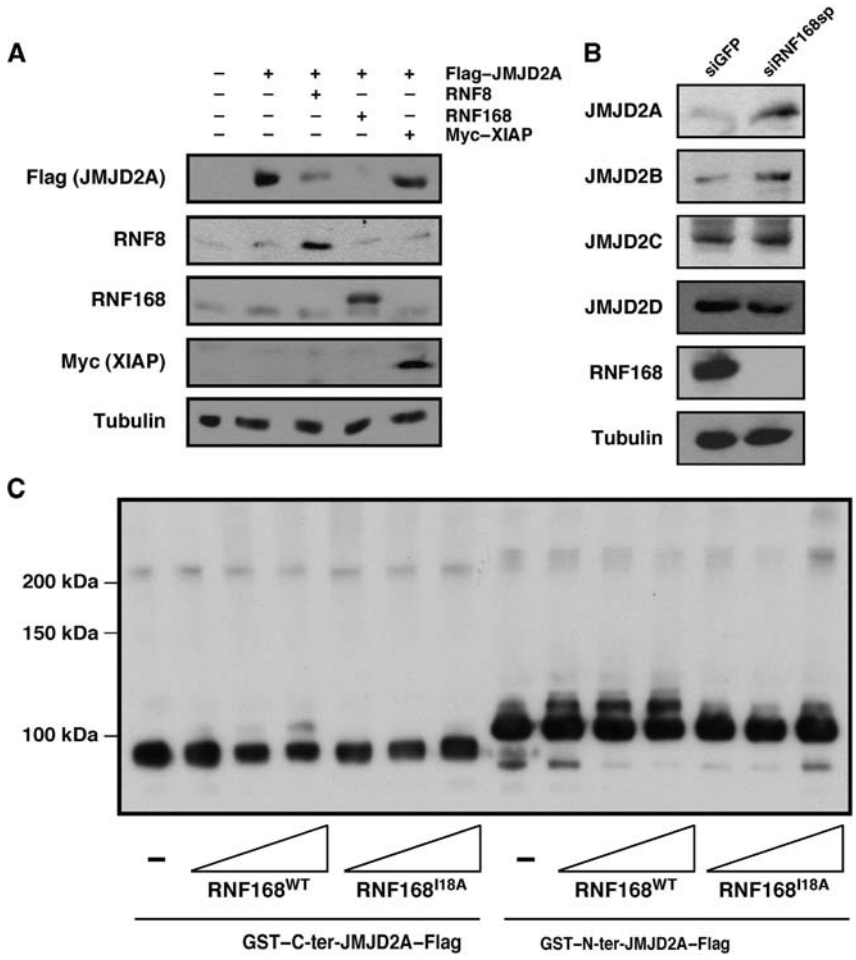

Figure 5 RNF168 directly ubiquitinates and regulates JMJD2A protein stability. (**A**) JMJD2A levels in U2OS cells transfected with plasmids expressing Flag–JMJD2A and RNF8, RNF168 or myc–XIAP. (**B**) Immunoblots of JMJD2 family members in U2OS cells transfected with siGFP or siRNF168sp. (**C**) *In vitro* ubiquitination of JMJD2A by RNF168. The Flag–GST-tagged JMJD2A C- and N-terminal regions were used as substrates for ubiquitination by purified RNF168 wild-type or RING domain mutant $RNF168^{I18A}$ in the presence of E1 (Uba1), E2 (UbcH5c) and ubiquitin. Increasing concentrations (0.1, 0.3 or 0.9 μM) of RNF168 or $RNF168^{I18A}$ were used. The ubiquitination reactions were analysed by anti-flag immunoblotting.

cells, while the single knockdown of JMJD2A had no impact on the formation of 53BP1 foci (Supplementary Figure S13). These results confirm the importance of JMJD2A/B degradation in the recruitment of 53BP1 at DNA damage sites.

Our findings imply that cells unable to degrade JMJD2A should display enhanced radiosensitivity. Indeed, the ectopic expression of wild-type JMJD2A or catalytic inactive $JMJD2A^{H188A}$ led to DNA damage hypersensitivity in U2OS cells, as assayed by a clonogenic survival assay (Figure 8E). However, the JMJD2A mutant disrupting the tandem tudor domain ($JMJD2A^{D939R}$) had no effect on cell survival following DNA damage (Figure 8E). These findings demonstrate the cellular role of JMJD2A in controlling the DNA damage response and 53BP1 recruitment. Our findings reveal that the RNF8-dependent degradation of JMJD2A following DNA damage exposes methylated histone marks for the recruitment of 53BP1 at DNA damage sites.

Discussion

53BP1 plays a crucial role in the preservation of genomic integrity (Morales *et al*, 2003) and the recruitment of 53BP1 at sites of DNA damage inhibits DNA end resection favouring non-homologous end joining (Bothmer *et al*, 2011). However, the molecular mechanism leading to the localization of 53BP1 at DNA breaks is still unclear. The dimethylation of H4K20 allows direct recognition by the tandem tudor domain of 53BP1 (Botuyan *et al*, 2006), but the event causing the exposure of H4K20(me2) was undefined. Since the lysine 20 of histone H4 is buried in stacked nucleosomes, it was initially thought that further modification of the chromatin might promote the accessibility of H4K20(me2), but nucleosomes are highly dynamic structures that allow exposure even of buried sites of chromatin (Li *et al*, 2005). Recently, it has been shown that the methyltransferase MMSET is recruited to DNA breaks to further enhance local methylation of H4K20 (Pei *et al*, 2011). Since most molecules of histone H4 are methylated on lysine 20 in untreated cells, this model of local increase of H4K20(me2) does not explain why 53BP1 is not constitutively bound to H4K20me2 throughout the chromatin in undamaged cells. Furthermore, this model does not integrate the requirement of the RNF8/RNF168 ubiquitination cascade. Based on the results obtained, we now propose a novel model linking histone methylation to RNF8 and

©2012 European Molecular Biology Organization

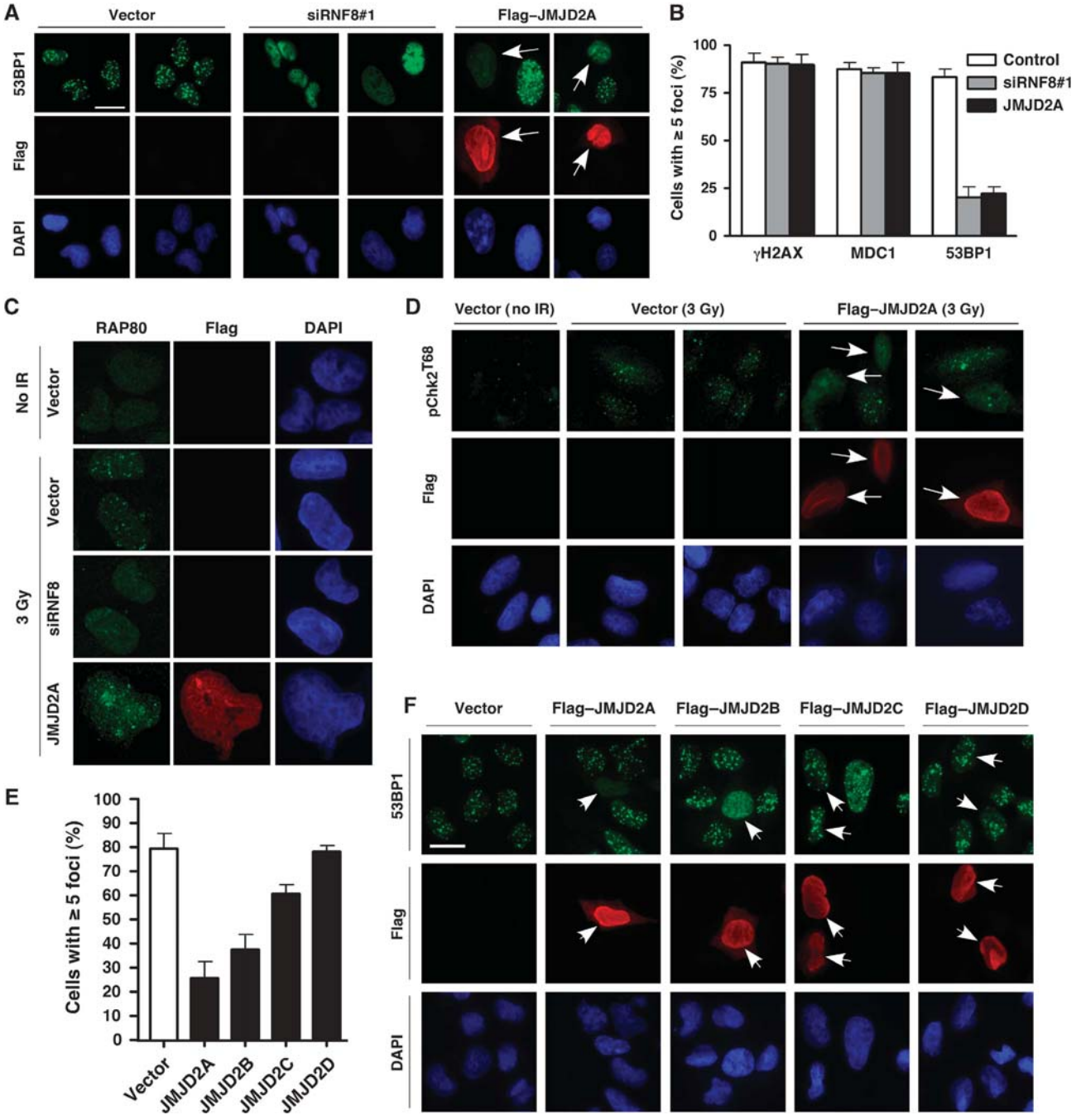

Figure 6 JMJD2A abrogates the recruitment of 53BP1 to DNA damaged sites. (**A**) Indirect immunofluorescence of 53BP1 and Flag–JMJD2A in U2OS cells transfected with siRNF8 or Flag–JMJD2A and fixed 1 h after irradiation with 3 Gy. Scale bars correspond to 20 μm and arrows indicate transfected cells. (**B**) Quantification of the γH2AX, MDC1 and 53BP1 foci in (**A**) and Supplementary Figure S6 is shown. These data represent the average and standard deviation of three independent counts of 100 cells each. (**C**) Indirect immunofluorescence of RAP80 and Flag–JMJD2A in U2OS cells transfected with siRNF8 or Flag–JMJD2A and fixed 1 h after IR (3 Gy). (**D**) Indirect immunofluorescence of phosphorylated Chk2 at threonine 68 and flag in U2OS transfected with an empty vector or pLPC Flag–JMJD2A and fixed 1 h after IR (3 Gy). (**E**) Quantification of the data presented in (**F**). (**F**) Indirect immunofluorescence of 53BP1 and flag in U2OS cells transfected with flag-tagged JMJD2A, JMJD2B, JMJD2C or JMJD2D, and fixed 1 h after exposure to IR (3 Gy). Scale bar corresponds to 20 μm and arrows indicate transfected cells.

RNF168. Taken together, the results presented here suggest that pre-existing methylated residues on H4 are bound by the tandem tudor of JMJD2A/B and that DNA damage triggers the degradation of JMJD2A/B to allow the exposure of methylated H4K20 for the binding of 53BP1. The RNF8- and RNF168-dependent ubiquitination cascade not only leads to the formation of polyubiquitin chains on histone H2A to allow the recruitment of RAP80/BRCA1, but also regulates the degradation of JMJD2A to give accessibility to 53BP1 to methylated histones (Figure 9). In support of our model, we described rapid degradation of JMJD2A (Figure 2E and F), which correlates with the kinetics of 53BP1 recruitment (Supplementary Figure S1). The relative affinity of JMJD2A/B for H4K20(me2) is also significantly higher than

 ©2012 European Molecular Biology Organization

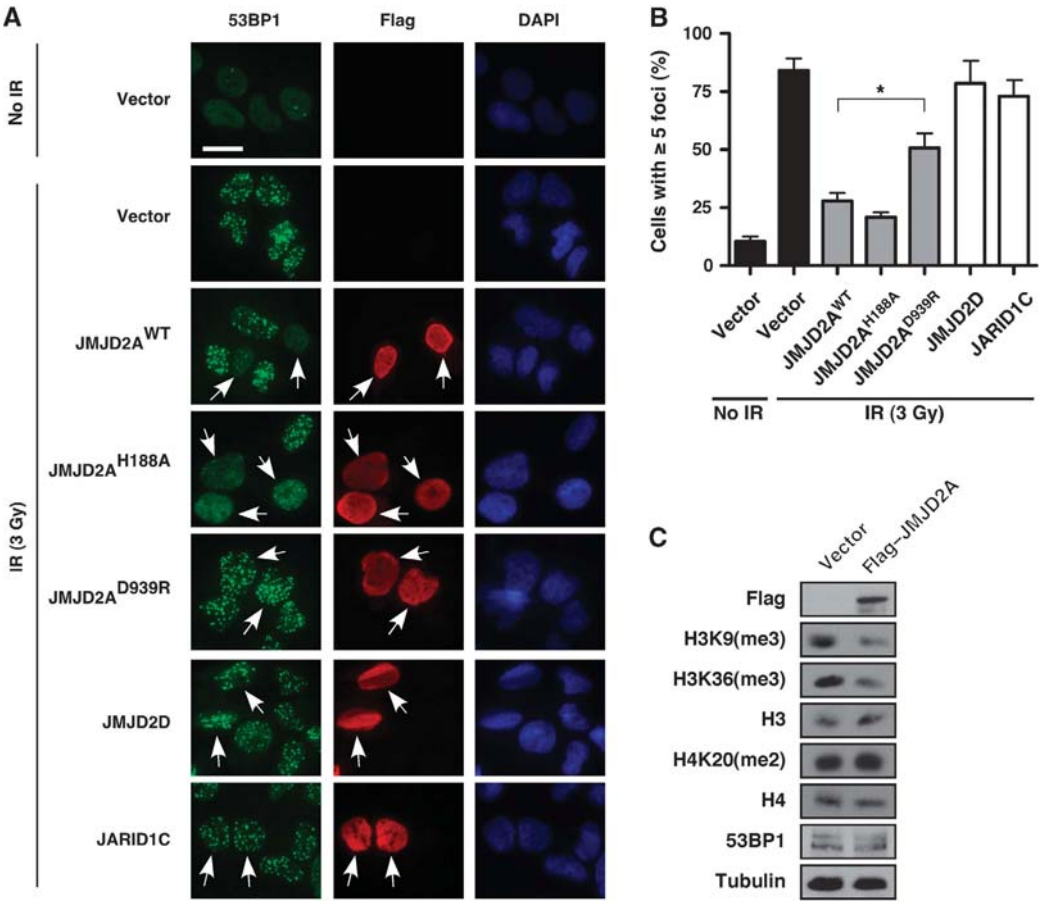

Figure 7 The integrity of the tandem tudor domain of JMJD2A is required to block 53BP1 foci formation. (**A**) Indirect immunofluorescence of 53BP1 and flag in U2OS cells transfected with different mutants of Flag–JMJD2A, Flag–JMJD2D or Flag–JARID1C and fixed 1 h after IR (3 Gy). Scale bar corresponds to 20 μm and arrows indicate transfected cells. (**B**) Quantification of the 53BP1 foci in cells presented in (**A**). Data represent the average and standard deviation of three independent counts of 100 cells. Asterisk corresponds to a $P<0.005$ using Student's *t*-test. (**C**) Immunoblots for different histone marks and 53BP1 in U2OS cells infected with a retroviral vector encoding Flag–JMJD2A or a control vector.

53BP1 (Figure 1D), suggesting that JMJD2A/B might preclude the recruitment of 53BP1. Furthermore, ectopic expression of JMJD2A/B competes with 53BP1 (Figure 6A, B, E and F; Supplementary Figure S7), indicating that JMJD2A/B must be efficiently degraded to ensure 53BP1 recruitment. JMJD2A and JMJD2B expression also caused enhanced sensitivity to DNA damage (Figure 8E). The presence of DNA repair defects caused by JMJD2A and JMJD2B, as opposed to other potential causes of enhanced sensitivity, remains to be addressed in future studies. We also identified a novel direct substrate of RNF8- and RNF168-mediated ubiquitination (Figures 3G and 5C), adding JMJD2A to the previously only known target, H2A. Our observation that both RNF8 and RNF168 are required for JMJD2A degradation is consistent with the data showing 53BP1 foci formation defects in RNF8- or RNF168-deficient cells. Finally, the rescue of 53BP1 foci in RNF8- and RNF168-depleted cells by the combined knockdown of JMJD2A and JMJD2B confirms that JMJD2A and JMJD2B are downstream targets of RNF8/RNF168 and that their degradation is required for efficient recruitment of 53BP1 (Figure 8A–D). Altogether, our results provide the first link between RNF8, RNF168, histone methylation and 53BP1 recruitment.

We observed a dramatic decrease in JMJD2A chromatin association after DNA damage (Figure 2G), suggesting that RNF8- and RNF168-dependent ubiquitination might also contribute to the release of JMJD2A from the chromatin and then allow protein degradation. Supporting this, we demonstrated that JMJD2A chromatin mobility is regulated by RNF8 (Supplementary Figure S3). Interestingly, the ubiquitin-selective segregase VCP/p97 stimulates the chromatin eviction of K48-linked ubiquitinated proteins (Ramadan *et al*, 2007; Verma *et al*, 2011). Furthermore, the recruitment of VCP/p97 to DNA breaks could promote the release of ubiquitinated JMJD2A to allow the efficient recruitment of 53BP1 (Meerang *et al*, 2011). The ATPase VCP/p97 promotes the removal of L3MBTL1, a protein able to bind to H4K20(me2), from DNA breaks, indicating that not only JMJD2A/B but also other H4K20(me2) binding proteins might regulate the recruitment of 53BP1 (Acs *et al*, 2011). However, JMJD2A ($K_D = 2.0\,\mu M$) and JMJD2B ($K_D = 27.7\,\mu M$) have significantly higher affinity for H4K20(me2) than both L3MBTL1 ($K_D = 211\,\mu M$; Min *et al*, 2007) and 53BP1 ($K_D = 50.8\,\mu M$), suggesting that JMJD2A/B release from chromatin is crucial to permit H4K20(me2) exposure and recruitment of 53BP1. The abundance of JMJD2A/B and L3MBTL1 in different tissues could also regulate 53BP1 foci formation. While JMJD2A is widely expressed in various tissues (Zhang *et al*, 2005), L3MBTL1 expression is restricted mainly to testis and brain (Qin *et al*, 2010).

©2012 European Molecular Biology Organization

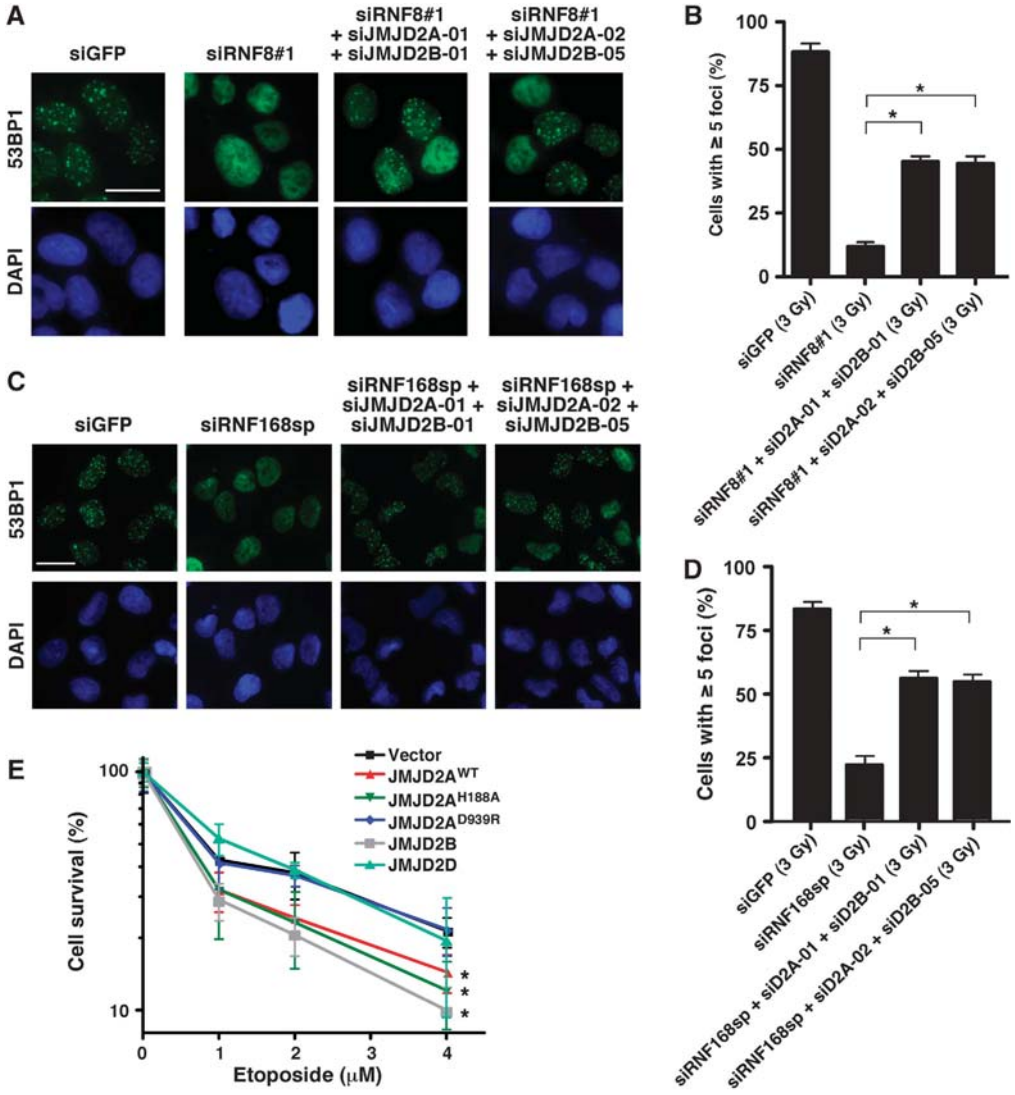

Figure 8 Combined knockdown of JMJD2A and JMJD2B rescues 53BP1 foci formation in RNF8- and RNF168-depleted cells. (**A**) Indirect immunofluorescence of 53BP1 in U2OS cells transfected with siRNF8#1 and different combinations of individual siJMJD2A and siJMJD2B, and fixed 1 h after IR (3 Gy). Scale bar corresponds to 20 μm. (**B**) Quantification of the 53BP1 foci in U2OS cells transfected with siRNF8#1 and different combinations of siJMJD2A and siJMJD2B. These data represent the average and standard deviation of three independent counts of 100 cells. Asterisks correspond to a $P<0.05$ using Student's *t*-test. (**C**) Indirect immunofluorescence of 53BP1 in U2OS cells transfected with a SMARTpool siRNF168sp and different combinations of individual siRNAs targeting JMJD2A and JMJD2B and fixed 1 h after IR (3 Gy). Scale bar corresponds to 20 μm. (**D**) Quantification of the 53BP1 foci in U2OS cells transfected with siRNF168sp and different combinations of individual siRNAs targeting JMJD2A and JMJD2B. These data represent the average and standard deviation of three independent counts of 100 cells. Asterisks correspond to a $P<0.01$ using Student's *t*-test. (**E**) Colony formation assay of U2OS cells stably infected with a control vector, wild-type or mutated JMJD2A, JMJD2B or JMJD2D and exposed to increasing amounts of etoposide for 3 h. The cells were then incubated for 14 days and stained using crystal violet. Colonies containing >50 cells were counted. The experiment was carried out in triplicate and asterisks represent a $P<0.05$ using the two-way ANOVA test.

Chromatin compaction was also found to modulate DNA repair processes. The dimethylation of H3K36 enhances the early recruitment of DNA repair factors, such as Ku70 and NBS1, and DNA repair through non-homologous end joining (Fnu *et al*, 2011). The local degradation of enzymes catalysing demethylation of H3K36, like JMJD2A and JMJD2B, could preserve the methylation state of histones thus increasing repair efficiency. Inhibiting the catalytic activity of JMJD2A/B through the RNF8- and RNF168-mediated degradation would provide another molecular mechanism leading to improved DNA repair efficacy by locally preserving methylation of H3K36 but also by promoting the recruitment of 53BP1.

Recently, JMD2A has been shown to be regulated by two different F-box ubiquitin ligases, FBXO22 and FbxL4 (Tan *et al*, 2011; Van Rechem *et al*, 2011). While the role of FbxL4-mediated degradation of JMJD2A has been associated with the regulation of the cell cycle, the role of FBXO22 is still unclear and might be related to development or differentiation. We now identify two RING finger ubiquitin ligases, RNF8 and RNF168, regulating JMJD2A ubiquitination in response of DNA damage and controlling the recruitment of 53BP1. Taken together, these findings show that JMJD2A protein levels are highly regulated by ubiquitination and the proteasome.

Ubiquitin and SUMO are key protein modifiers localizing to DNA breaks and regulating the formation of protein–protein interactions after DNA damage (Huen *et al*, 2007; Kolas *et al*, 2007; Mailand *et al*, 2007; Galanty *et al*, 2009;

 ©2012 European Molecular Biology Organization

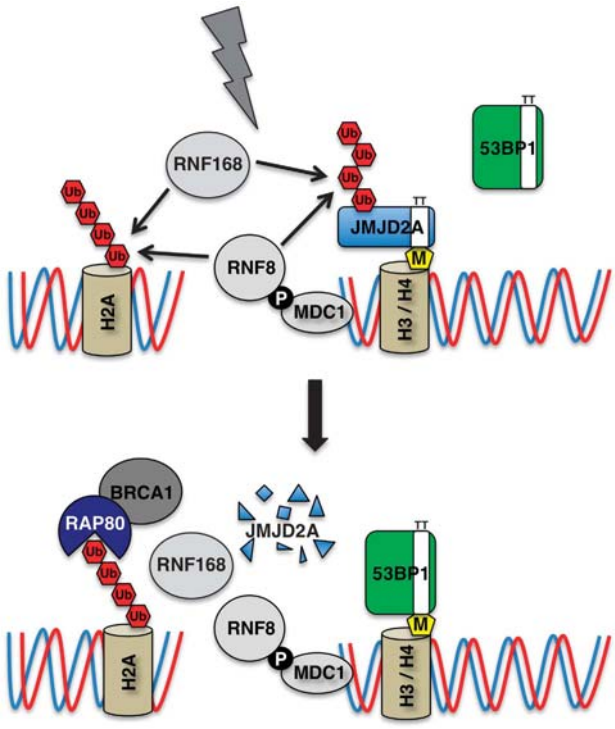

Figure 9 The RNF8- and RNF168-mediated degradation of JMJD2A regulates the formation of 53BP1 foci. Schematic model of the role of RNF8/RNF168 in the degradation of JMJD2A and the formation of 53BP1 and BRCA1/RAP80 foci. In undamaged cells, JMJD2A binds H4K20(me2) via its tandem tudor domain. Following DNA damage, RNF8 initiates the ubiquitination of JMJD2A which is further amplified by RNF168 to ensure efficient and local degradation of JMJD2A leading to the exposure of H4K20(me2). 53BP1, which can bind H4K20(me2) with a lower affinity than JMJD2A/B, can now interact with H4K20(me2) through its tandem tudor to accumulate at sites of DNA damage. RNF8 and RNF168 trigger two types of ubiquitination cascades leading independently to the recruitment of RAP80 and 53BP1.

Morris *et al*, 2009), but the role of ubiquitin-dependent degradation in the DNA damage response remains undefined. Our study highlights the role of ubiquitin and protein degradation in the dynamics of 53BP1 foci formation in response to DNA damage. We also demonstrate a common activity of the RNF8 and RNF168 ubiquitination cascade. Previous literature suggested for H2A ubiquitination that RNF8 is required to initiate histone ubiquitination, but RNF168 is necessary to amplify the ubiquitin conjugation (Doil *et al*, 2009; Stewart *et al*, 2009). Our results describe a joint action during JMJD2A ubiquitination and degradation after DNA breaks confirming a conserved joint activity for RNF8- and RNF168-mediated ubiquitination. Although H4K20(me2) has been reported to increase at DNA breaks (Pei *et al*, 2011), our model is consistent with the pre-existence of H4K20(me2) observed in ~85% of all H4 molecules in undamaged cells (Schotta *et al*, 2008). The tighter affinity of JMJD2A and JMJD2B for H4K20(me2) compared with 53BP1 suggests that in the absence of their complete degradation, JMJD2A and JMJD2B would remain loaded on chromatin instead of allowing formation of 53BP1 foci (Figure 6A and F). The local degradation of JMJD2A at sites of RNF8/RNF168 recruitment would allow confined and precise exposure of H4K20(me2) to ensure efficient and restricted 53BP1 accumulation. In addition, we identify JMJD2A as a link between the RNF8-mediated ubiquitination cascade and the recruitment of 53BP1 to methylated histones at damaged sites.

Materials and methods

Cells, plasmids, site-directed mutagenesis and retroviral infections

Human osteosarcoma cells U2OS (ATCC) were cultured in Dulbecco's modified Eagle medium (DMEM) supplemented with 10% fetal bovine serum (FBS) (Hyclone) and antibiotics. The plasmids encoding RNF8 and RNF168 were previously described (Kolas *et al*, 2007; Stewart *et al*, 2009). The pLPC-puro Flag–JMJD2A, Flag–JMJD2B and Flag–JMJD2D were generated by introducing an amino-terminal flag epitope by PCR and cloning into pLPC-puro. The pCMV6-myc-DDK-JMJD2C was obtained from OriGene. Retroviral infections were carried out as previously described (Mallette *et al*, 2007). Site-directed mutagenesis was performed using the Quick Change site-directed mutagenesis kit (Stratagene).

Isothermal titration calorimetry

The ITC measurements were carried out at 10°C using a VP-ITC titration calorimeter (GE Healthcare). 53BP1-tudor and JMJD2A-tudor were prepared as previously published (Botuyan *et al*, 2006). The DNA sequence of the hybrid tudor domains of murine JMJD2B (JMJD2B-tudor, residues 898–1009) was cloned into an expression plasmid derived from pET15b (Novagen) encoding a tobacco etch virus (TEV) protease-cleavable N-terminal $(His)_6$ tag. The protein was produced in BL21(DE3) *E. coli* cells (Novagen). Bacteria were grown at 37°C to an optical density at 600 nm of about 0.9 and then transferred to 18°C. Protein production was induced with 1 mM final concentration of isopropyl β-D-1 thiogalactopyranoside after 45 min at 18°C and allowed to continue overnight. Cells were harvested and ruptured using an Emulsiflex C-5 high-pressure homogenizer (Avestin, Inc.) and the protein purified by Ni^{2+}-NTA affinity chromatography following a standard protocol (Qiagen). The $(His)_6$ tag was cleaved by overnight digestion with TEV protease at room temperature, leaving the GHM sequence at the N-terminus of JMJD2B-tudor. The protein was further purified by size exclusion chromatography using a Superdex 75 column (GE Healthcare). The $H4K_C20me2$ peptide (residues 12–25) was prepared from expression in *E. coli* and chemical installation of a methyllysine analogue using a previously reported procedure (Simon *et al*, 2007; Cui *et al*, 2009). Protein and peptide samples were in 50 mM Tris–HCl, pH 7.5 and 50 mM NaCl. $H4K_C20me2$, placed in the calorimeter injection syringe at concentrations ranging from 1 to 2 mM, was delivered to the reaction cell containing 53BP1-tudor, JMJD2A-tudor or JMJD2B-tudor at concentrations of 30 μM. Data were analysed by LevenbergMarquardt non-linear regression fit of the ITC isotherms using a model corresponding to one independent binding event.

Western blot analysis and immunofluorescence

For western blotting, cells were lysed in 20 mM Tris (pH 7.5), 150 mM NaCl, 1 mM EDTA, 1 mM EGTA, 1% Triton X-100 and EDTA-free protease inhibitors (Complete, Roche) and sonicated three times for 10 s each. Proteins were separated on SDS–PAGE and transferred onto nitrocellulose membranes (Bio-Rad). Primary antibodies used were anti-H3K36(me3) (9763, Cell Signaling; 1:1000), anti-H3K9(me3) (AR-0170, Lake Placid Biologicals; 1:2500), anti-H3 (AR-0144, Lake Placid Biologicals; 1:5000), anti-H4K20(me2) (05-672, Upstate; 1:2000), anti-H4 (07-108, Upstate; 1:5000), anti-γH2AX (39117, ActiveMotif; 1:1000), anti-$pChk2^{T68}$ (2661, Cell Signaling; 1:1000), anti-α-Tubulin (B-5-1-2, Sigma; 1:5000), anti-pan-Actin (C4, Millipore; 1:5000), anti-flag (M2, Sigma; 1:4000), anti-GFP (Roche; 1:1000), anti-JMJD2A (NB110-40585, Novus Biologicals; 1:1000), anti-JMJD2B (NB100-74605, Novus Biologicals; 1:2000), anti-JMJD2C (NB110-38884, Novus Biologicals; 1:1000), anti-HA (12CA5, 1:1000), anti-RNF8 (kind gift of Dr Junjie Chen, Department of Therapeutic Radiology, Yale University School of Medicine, New Haven, CT, USA; 1:500) and anti-53BP1 (NB100-304, Novus Biologicals; 1:1000).

For immunofluorescence, U2OS cells transfected with pLPC-puro Flag–JMJD2A or siRNA targeting RNF8 were grown on coverslips in

©2012 European Molecular Biology Organization

6-well plates. Cells were fixed 1 h after IR or doxorubicin treatment in 4% paraformaldehyde for 15 min and permeabilized with PBS, 3% BSA, 0.2% Triton X-100 for 5 min. Cells were then washed three times with PBS, 3% BSA and stained with anti-flag (M2, Sigma; 1:400), anti-JMJD2A (NB110-40585, Novus Biologicals; 1:200 and 3393, Cell Signaling; 1:200), anti-53BP1 (NB100-304, Novus Biologicals; 1:200), anti-γH2AX (JBW301, Upstate; 1:200), anti-ubiquitin K48 specific (APU2, Millipore; 1:200), anti-ubiquitin K63 specific (APU3, Millipore; 1:200), anti-pChk2^{T68} (2661, Cell Signaling; 1:200), anti-MDC1 (NB100-397A, Novus Biologicals; 1:200) or anti-RAP80 (A300-763A, Bethyl; 1:200). Secondary antibodies used were AlexaFluor488- or AlexaFluor546-conjugated secondary antibodies (Molecular Probes; 1:1000).

Protein stability assay

For half-life measurement, U2OS cells were pre-treated with 100 μg/ml cycloheximide and 40 μg/ml chloramphenicol for 1 h. Cells were then left untreated or treated with 2 μM doxorubicin and harvested at the indicated time periods.

Chromatin isolation

Chromatin isolation by small-scale biochemical fractionation was performed as previously described (Mendez and Stillman, 2000).

siRNA transfections

siRNAs targeting GFP (5′-AAC ACU UGU CAC UAC UUU CUC-3′), RNF8 (siRNF8#1: 5′-CAG AGA AGC UUA CAG AUG UUU-3′, siRNF8#2: 5′-AGA AUG AGC UCC AAU GUA UUU-3′) (as previously described; Huen *et al*, 2007), RNF168 (siGENOME SMARTpool), JMJD2A (siGENOME SMARTpool and individuals), JMJD2B (siGENOME SMARTpool and individuals) and JMJD2C (siGENOME SMARTpool) were all purchased from Thermo-Scientific (Dharmacon). All siRNA transfections were performed with 25 nM siRNA duplexes using Lipofectamine RNAiMAX reagent (Invitrogen) in a reverse transfection mode according to manufacturer's protocol.

Protein expression and purification

Recombinant full-length human RNF8 was cloned in an N-terminal GST-3C pFastbac vector, and expressed in Sf21 insect cells. The plasmid containing the cDNA of RNF168 (a gift of J Lukas) was expressed in *E. coli* as a GST-fusion protein. Mutations at the E2-binding interface of the RING domain of RNF8 (RNF8^{I405A}) and RNF168 (RNF168^{I18A}) greatly reduced the ubiquitin ligase activity (Brzovic *et al*, 2003). The proteins were purified on glutathione beads (GE Healthcare) in a buffer containing 50 mM HEPES pH 8.0, 500 mM NaCl, 10% glycerol, 1 μM $ZnCl_2$, 1 mM TCEP for RNF8, while a buffer containing 50 mM HEPES pH 8.0, 200 mM NaCl, 10% glycerol, 1 μM $ZnCl_2$, 1 mM TCEP was used for RNF168. After elution with 50 mM glutathione, the protein was cleaved in solution with 3C protease. Protein was diluted to 50 mM NaCl and purified by Heparin affinity chromatography (GE Healthcare). The RING domain of human RNF8, residues 351–485, was expressed in *E. coli* as a GST-fusion protein. Protein was purified over glutathione beads in a buffer containing 50 mM HEPES pH 8.0, 50 mM NaCl, 10% glycerol, 1 μM $ZnCl_2$, 1 mM TCEP. After elution with 50 mM glutathione, the protein was cleaved in solution using 3C protease and purified on an S75 Superdex column (GE Healthcare) in tandem with a GSH column (1 ml, GE Healthcare), followed by ion exchange chromatography on a ResourceQ column. Proteins were concentrated to 1–10 mg/ml and stored at −80°C in lysis buffer. Flag-tagged N-terminal JMJD2A (residues 1–532) and C-terminal JMJD2A (residues 533–1064) were cloned into pGEX-5X3, and proteins were purified in *E. coli* using standard GST protein purification. Uba1, UbcH5c and ubiquitin were prepared as previously described (Buchwald *et al*, 2006).

Ubiquitination assays

For *in vivo* ubiquitination, U2OS cells were co-transfected with pLPC Flag–JMJD2A and pcDNA HA–ubiquitin. Twenty-four hours following transfection, cells were treated or not with 5 μM MG132 for 16 h. Cells were then lysed in 20 mM Tris (pH 7.5), 150 mM NaCl, 1 mM EDTA, 1 mM EGTA, 1% Triton X-100, 10 mM N-ethylmaleimide and EDTA-free protease inhibitors (Complete, Roche) and sonicated three times for 10 s each. Cell lysates were incubated with anti-flag M2 (Sigma) overnight at 4°C. A mixture of protein A/G-agarose was used to immunoprecipitate the complexes and proteins were resolved by SDS–PAGE.

For *in vitro* ubiquitination, purified human Uba1 (600 nM) was mixed with UbcH5c (500 nM), the E3 ligases (2 μM), ubiquitin (94 μM), ATP (3 mM) and different constructs of Flag–GST–JMJD2A or Flag–GST. The reactions were incubated at 32°C for 3 h in a buffer containing 50 mM Tris/HCl (pH 7.5), 100 mM NaCl, 10 mM $MgCl_2$, 1 μM $ZnCl_2$, 1 mM TCEP. The reactions were stopped using SDS loading buffer, then samples were boiled and loaded on 4–12% NuPAGE gels (Invitrogen). Detection was performed by western blot using anti-flag antibody (M2, Sigma-Aldrich; 1:5000) in 5% milk and blotted onto nitrocellulose.

Biotinylated peptides pulldown

Peptide pulldowns were performed as previously described (Kim *et al*, 2006). Briefly, biotinylated peptides (1 μg) were immobilized on streptavidine beads in 500 μl of binding buffer (50 mM Tris–HCl pH 7.5, 15 mM NaCl, 1 mM EDTA, 2 mM DTT and 0.5% NP-40) overnight at 4°C. Following three washes with binding buffer, 1 μg of GST-purified fusion protein corresponding to the tandem tudor domain of JMJD2A or 53BP1 was incubated with the beads for 2.5 h at 4°C. After five washes with binding buffer, proteins were boiled in Laemmli buffer and analysed by SDS–PAGE. Detection was performed by western blot using anti-GST antibody (HRP) (ab3416, Abcam; 1:5000).

RT–qPCR

In all, 2 μg of total RNA was reverse transcribed in a final volume of 20 μl using the High Capacity cDNA Reverse Transcription Kit with random primers (Applied Biosystems) as described by the manufacturer. Gene expression level for endogenous controls was determined using pre-validated Taqman Gene Expression Assays (Applied Biosystems). qPCRs in 384-well plate were performed using 1.5 μl of cDNA samples (5–25 ng), 5 μl of the TaqMan Fast Universal PCR Master Mix (Applied Biosystems), 0.5 μl of the TaqMan Gene Expression Assay (20 ×) and 3 μl of water in a total volume of 10 μl. The following assays were used as endogenous control: GAPDH (glyceraldehyde-3-phosphate dehydrogenase), TBP (TATA binding protein), HPRT1 (hypoxanthine guanine phosphoribosyl transferase) and ACTB (β-actin). Gene expression level for target genes was determined using assays designed with the Universal Probe Library from Roche (http://www.universalprobelibrary.com). qPCRs for 384-well plate format were performed using 1.5 μl of cDNA samples (5–25 ng), 5 μl of the TaqMan Fast Universal PCR Master Mix (Applied Biosystems), 2 μM of each primer and 1 μM of a UPL probe in a total volume of 10 μl. The ABI PRISM® 7900HT Sequence Detection System (Applied Biosystems) was used to detect the amplification level and was programmed with an initial step of 3 min at 95°C, followed by 40 cycles of 5 s at 95°C and 30 s at 60°C. All reactions were run in triplicate and the average values of Cts were used for quantification. The relative quantification of target genes was determined using the ΔΔCT method.

Fluorescence recovery after photobleaching

Jmjd2a–mEGFP and Jmjd2b–EGFP were introduced into RNF8$^{+/+}$ and RNF8$^{-/-}$ cells (Wu *et al*, 2009) by transient transfection and relative mobility was analysed using FRAP (Raghuram *et al*, 2010).

Supplementary data

Supplementary data are available at *The EMBO Journal* Online (http://www.embojournal.org).

Acknowledgements

We thank Daniel Durocher for reagents, critical reading of the manuscript and helpful suggestions. We also thank Junjie Chen, Michael SY Huen, Jiri Lukas, Mark T Bedford and Michihiko Ito for reagents, and members of the Richard laboratory for helpful comments. We thank Raphaëlle Lambert and the Genomics core facility of the Institute for Research in Immunology and Cancer (IRIC, Montréal, Canada). We are grateful to Émilie Bolduc for technical assistance with the ionizing radiation experiments. FAM received postdoctoral fellowships from the Fonds de Recherche en Santé du Québec (FRSQ), the Canadian Institutes of Health Research (CIHR) and the Terry Fox Foundation through an award from the National Cancer Institute of Canada (NCIC). SR is a recipient of a

 ©2012 European Molecular Biology Organization

Chercheur-National Award from the FRSQ. This work was funded by CIHR grant MOP-67070 to SR, NIH grant CA132878 to GM, Alberta Cancer Foundation grant 24955 to MJH and by KWF grant 2006-3476 to TKS.

Author contributions: FAM and SR analysed the data, conceived the study and wrote the paper. FAM initiated the project and performed all the experiments except isothermal titration calorimetry performed by GC and GM, FRAP performed by LCY and MJH, and *in vitro* ubiquitination assays performed by FM and TKS.

Conflict of interest

The authors declare that they have no conflict of interest.

References

Acs K, Luijsterburg MS, Ackermann L, Salomons FA, Hoppe T, Dantuma NP (2011) The AAA-ATPase VCP/p97 promotes 53BP1 recruitment by removing L3MBTL1 from DNA double-strand breaks. *Nat Struct Mol Biol* **18:** 1345–1350

Bekker-Jensen S, Danielsen JR, Fugger K, Gromova I, Nerstedt A, Bartek J, Lukas J, Mailand N (2010) HERC2 coordinates ubiquitin-dependent assembly of DNA repair factors on damaged chromosomes. *Nat Cell Biol* **12:** 80–86; sup pp 1–12

Bekker-Jensen S, Lukas C, Melander F, Bartek J, Lukas J (2005) Dynamic assembly and sustained retention of 53BP1 at the sites of DNA damage are controlled by Mdc1/NFBD1. *J Cell Biol* **170:** 201–211

Bothmer A, Robbiani DF, Di Virgilio M, Bunting SF, Klein IA, Feldhahn N, Barlow J, Chen HT, Bosque D, Callen E, Nussenzweig A, Nussenzweig MC (2011) Regulation of DNA end joining, resection, and immunoglobulin class switch recombination by 53BP1. *Mol Cell* **42:** 319–329

Botuyan MV, Lee J, Ward IM, Kim JE, Thompson JR, Chen J, Mer G (2006) Structural basis for the methylation state-specific recognition of histone H4-K20 by 53BP1 and Crb2 in DNA repair. *Cell* **127:** 1361–1373

Brzovic PS, Keeffe JR, Nishikawa H, Miyamoto K, Fox III D, Fukuda M, Ohta T, Klevit R (2003) Binding and recognition in the assembly of an active BRCA1/BARD1 ubiquitin-ligase complex. *Proc Natl Acad Sci USA* **100:** 5646–5651

Buchwald G, van der Stoop P, Weichenrieder O, Perrakis A, van Lohuizen M, Sixma TK (2006) Structure and E3-ligase activity of the Ring-Ring complex of polycomb proteins Bmi1 and Ring1b. *EMBO J* **25:** 2465–2474

Cloos PA, Christensen J, Agger K, Maiolica A, Rappsilber J, Antal T, Hansen KH, Helin K (2006) The putative oncogene GASC1 demethylates tri- and dimethylated lysine 9 on histone H3. *Nature* **442:** 307–311

Couture JF, Collazo E, Ortiz-Tello PA, Brunzelle JS, Trievel RC (2007) Specificity and mechanism of JMJD2A, a trimethyllysine-specific histone demethylase. *Nat Struct Mol Biol* **14:** 689–695

Cui G, Botuyan MV, Mer G (2009) Preparation of recombinant peptides with site- and degree-specific lysine (13)C-methylation. *Biochemistry* **48:** 3798–3800

Doil C, Mailand N, Bekker-Jensen S, Menard P, Larsen DH, Pepperkok R, Ellenberg J, Panier S, Durocher D, Bartek J, Lukas J, Lukas C (2009) RNF168 binds and amplifies ubiquitin conjugates on damaged chromosomes to allow accumulation of repair proteins. *Cell* **136:** 435–446

Fnu S, Williamson EA, De Haro LP, Brenneman M, Wray J, Shaheen M, Radhakrishnan K, Lee SH, Nickoloff JA, Hromas R (2011) Methylation of histone H3 lysine 36 enhances DNA repair by nonhomologous end-joining. *Proc Natl Acad Sci USA* **108:** 540–545

Galanty Y, Belotserkovskaya R, Coates J, Polo S, Miller KM, Jackson SP (2009) Mammalian SUMO E3-ligases PIAS1 and PIAS4 promote responses to DNA double-strand breaks. *Nature* **462:** 935–939

Goldberg M, Stucki M, Falck J, D'Amours D, Rahman D, Pappin D, Bartek J, Jackson SP (2003) MDC1 is required for the intra-S-phase DNA damage checkpoint. *Nature* **421:** 952–956

Huang Y, Fang J, Bedford MT, Zhang Y, Xu RM (2006) Recognition of histone H3 lysine-4 methylation by the double tudor domain of JMJD2A. *Science* **312:** 748–751

Huen MS, Grant R, Manke I, Minn K, Yu X, Yaffe MB, Chen J (2007) RNF8 transduces the DNA-damage signal via histone ubiquitylation and checkpoint protein assembly. *Cell* **131:** 901–914

Jacquemont C, Taniguchi T (2007) Proteasome function is required for DNA damage response and fanconi anemia pathway activation. *Cancer Res* **67:** 7395–7405

Kim J, Daniel J, Espejo A, Lake A, Krishna M, Xia L, Zhang Y, Bedford MT (2006) Tudor, MBT and chromo domains gauge the degree of lysine methylation. *EMBO Rep* **7:** 397–403

Klose RJ, Yamane K, Bae Y, Zhang D, Erdjument-Bromage H, Tempst P, Wong J, Zhang Y (2006) The transcriptional repressor JHDM3A demethylates trimethyl histone H3 lysine 9 and lysine 36. *Nature* **442:** 312–316

Kolas NK, Chapman JR, Nakada S, Ylanko J, Chahwan R, Sweeney FD, Panier S, Mendez M, Wildenhain J, Thomson TM, Pelletier L, Jackson SP, Durocher D (2007) Orchestration of the DNA-damage response by the RNF8 ubiquitin ligase. *Science* **318:** 1637–1640

Lee J, Thompson JR, Botuyan MV, Mer G (2008) Distinct binding modes specify the recognition of methylated histones H3K4 and H4K20 by JMJD2A-tudor. *Nat Struct Mol Biol* **15:** 109–111

Li G, Levitus M, Bustamante C, Widom J (2005) Rapid spontaneous accessibility of nucleosomal DNA. *Nat Struct Mol Biol* **12:** 46–53

Lou Z, Minter-Dykhouse K, Franco S, Gostissa M, Rivera MA, Celeste A, Manis JP, van Deursen J, Nussenzweig A, Paull TT, Alt FW, Chen J (2006) MDC1 maintains genomic stability by participating in the amplification of ATM-dependent DNA damage signals. *Mol Cell* **21:** 187–200

Lou Z, Minter-Dykhouse K, Wu X, Chen J (2003) MDC1 is coupled to activated CHK2 in mammalian DNA damage response pathways. *Nature* **421:** 957–961

Mailand N, Bekker-Jensen S, Faustrup H, Melander F, Bartek J, Lukas C, Lukas J (2007) RNF8 ubiquitylates histones at DNA double-strand breaks and promotes assembly of repair proteins. *Cell* **131:** 887–900

Mallette FA, Gaumont-Leclerc MF, Ferbeyre G (2007) The DNA damage signaling pathway is a critical mediator of oncogene-induced senescence. *Genes Dev* **21:** 43–48

Meerang M, Ritz D, Paliwal S, Garajova Z, Bosshard M, Mailand N, Janscak P, Hubscher U, Meyer H, Ramadan K (2011) The ubiquitin-selective segregase VCP/p97 orchestrates the response to DNA double-strand breaks. *Nat Cell Biol* **13:** 1376–1382

Mendez J, Stillman B (2000) Chromatin association of human origin recognition complex, cdc6, and minichromosome maintenance proteins during the cell cycle: assembly of prereplication complexes in late mitosis. *Mol Cell Biol* **20:** 8602–8612

Min J, Allali-Hassani A, Nady N, Qi C, Ouyang H, Liu Y, MacKenzie F, Vedadi M, Arrowsmith CH (2007) L3MBTL1 recognition of mono- and dimethylated histones. *Nat Struct Mol Biol* **14:** 1229–1230

Morales JC, Xia Z, Lu T, Aldrich MB, Wang B, Rosales C, Kellems RE, Hittelman WN, Elledge SJ, Carpenter PB (2003) Role for the BRCA1 C-terminal repeats (BRCT) protein 53BP1 in maintaining genomic stability. *J Biol Chem* **278:** 14971–14977

Morris JR, Boutell C, Keppler M, Densham R, Weekes D, Alamshah A, Butler L, Galanty Y, Pangon L, Kiuchi T, Ng T, Solomon E (2009) The SUMO modification pathway is involved in the BRCA1 response to genotoxic stress. *Nature* **462:** 886–890

Ng SS, Kavanagh KL, McDonough MA, Butler D, Pilka ES, Lienard BM, Bray JE, Savitsky P, Gileadi O, von Delft F, Rose NR, Offer J, Scheinost JC, Borowski T, Sundstrom M, Schofield CJ, Oppermann U (2007) Crystal structures of histone demethylase JMJD2A reveal basis for substrate specificity. *Nature* **448:** 87–91

Pei H, Zhang L, Luo K, Qin Y, Chesi M, Fei F, Bergsagel PL, Wang L, You Z, Lou Z (2011) MMSET regulates histone H4K20 methylation and 53BP1 accumulation at DNA damage sites. *Nature* **470:** 124–128

Plans V, Scheper J, Soler M, Loukili N, Okano Y, Thomson TM (2006) The RING finger protein RNF8 recruits UBC13 for lysine 63-based self polyubiquitylation. *J Cell Biochem* **97:** 572–582

Qin J, Van Buren D, Huang HS, Zhong L, Mostoslavsky R, Akbarian S, Hock H (2010) Chromatin protein L3MBTL1 is

©2012 European Molecular Biology Organization

dispensable for development and tumor suppression in mice. *J Biol Chem* **285:** 27767–27775

Raghuram N, Carrero G, Stasevich TJ, McNally JG, Th'ng J, Hendzel MJ (2010) Core histone hyperacetylation impacts cooperative behavior and high-affinity binding of histone H1 to chromatin. *Biochemistry* **49:** 4420–4431

Ramadan K, Bruderer R, Spiga FM, Popp O, Baur T, Gotta M, Meyer HH (2007) Cdc48/p97 promotes reformation of the nucleus by extracting the kinase Aurora B from chromatin. *Nature* **450:** 1258–1262

Sakasai R, Tibbetts R (2008) RNF8-dependent and RNF8-independent regulation of 53BP1 in response to DNA damage. *J Biol Chem* **283:** 13549–13555

Sanders SL, Portoso M, Mata J, Bahler J, Allshire RC, Kouzarides T (2004) Methylation of histone H4 lysine 20 controls recruitment of Crb2 to sites of DNA damage. *Cell* **119:** 603–614

Schotta G, Sengupta R, Kubicek S, Malin S, Kauer M, Callen E, Celeste A, Pagani M, Opravil S, De La Rosa-Velazquez IA, Espejo A, Bedford MT, Nussenzweig A, Busslinger M, Jenuwein T (2008) A chromatin-wide transition to H4K20 monomethylation impairs genome integrity and programmed DNA rearrangements in the mouse. *Genes Dev* **22:** 2048–2061

Shroff R, Arbel-Eden A, Pilch D, Ira G, Bonner WM, Petrini JH, Haber JE, Lichten M (2004) Distribution and dynamics of chromatin modification induced by a defined DNA double-strand break. *Curr Biol* **14:** 1703–1711

Simon MD, Chu F, Racki LR, de la Cruz CC, Burlingame AL, Panning B, Narlikar GJ, Shokat KM (2007) The site-specific installation of methyl-lysine analogs into recombinant histones. *Cell* **128:** 1003–1012

Stewart GS, Panier S, Townsend K, Al-Hakim AK, Kolas NK, Miller ES, Nakada S, Ylanko J, Olivarius S, Mendez M, Oldreive C, Wildenhain J, Tagliaferro A, Pelletier L, Taubenheim N, Durandy A, Byrd PJ, Stankovic T, Taylor AM, Durocher D (2009) The RIDDLE syndrome protein mediates a ubiquitin-dependent signaling cascade at sites of DNA damage. *Cell* **136:** 420–434

Stewart GS, Wang B, Bignell CR, Taylor AM, Elledge SJ (2003) MDC1 is a mediator of the mammalian DNA damage checkpoint. *Nature* **421:** 961–966

Stucki M, Clapperton JA, Mohammad D, Yaffe MB, Smerdon SJ, Jackson SP (2005) MDC1 directly binds phosphorylated histone H2AX to regulate cellular responses to DNA double-strand breaks. *Cell* **123:** 1213–1226

Tan MK, Lim HJ, Harper JW (2011) SCF(FBXO22) regulates histone H3 lysine 9 and 36 methylation levels by targeting histone demethylase KDM4A for ubiquitin-mediated proteasomal degradation. *Mol Cell Biol* **31:** 3687–3699

van Attikum H, Gasser SM (2009) Crosstalk between histone modifications during the DNA damage response. *Trends Cell Biol* **19:** 207–217

Van Rechem C, Black JC, Abbas T, Allen A, Rinehart CA, Yuan GC, Dutta A, Whetstine JR (2011) The SKP1-Cul1-F-box and leucine-rich repeat protein 4 (SCF-FbxL4) ubiquitin ligase regulates lysine demethylase 4A (KDM4A)/Jumonji domain-containing 2A (JMJD2A) protein. *J Biol Chem* **286:** 30462–30470

Verma R, Oania R, Fang R, Smith GT, Deshaies RJ (2011) Cdc48/p97 mediates UV-dependent turnover of RNA Pol II. *Mol Cell* **41:** 82–92

Wang B, Elledge SJ (2007) Ubc13/Rnf8 ubiquitin ligases control foci formation of the Rap80/Abraxas/Brca1/Brcc36 complex in response to DNA damage. *Proc Natl Acad Sci USA* **104:** 20759–20763

Wang B, Matsuoka S, Carpenter PB, Elledge SJ (2002) 53BP1, a mediator of the DNA damage checkpoint. *Science* **298:** 1435–1438

Whetstine JR, Nottke A, Lan F, Huarte M, Smolikov S, Chen Z, Spooner E, Li E, Zhang G, Colaiacovo M, Shi Y (2006) Reversal of histone lysine trimethylation by the JMJD2 family of histone demethylases. *Cell* **125:** 467–481

Wu J, Huen MS, Lu LY, Ye L, Dou Y, Ljungman M, Chen J, Yu X (2009) Histone ubiquitination associates with BRCA1-dependent DNA damage response. *Mol Cell Biol* **29:** 849–860

Zhang D, Yoon HG, Wong J (2005) JMJD2A is a novel N-CoR-interacting protein and is involved in repression of the human transcription factor achaete scute-like homologue 2 (ASCL2/Hash2). *Mol Cell Biol* **25:** 6404–6414

 ©2012 European Molecular Biology Organization